

## OPTICAL INDICES OF PYROLYTIC TIN-OXIDE GLASS

K. VON ROTTKAY, M. RUBIN

Lawrence Berkeley National Laboratory,  
University of California, MS 2-300, 1 Cyclotron Road, Berkeley CA 94720,  
KvonRottkay@lbl.gov, MDRubin@lbl.gov

### ABSTRACT

SnO<sub>2</sub>:F is a widely used transparent conductor and commercially available in a multilayer structure as Tech glass. Current applications include photovoltaics, electrochromics and displays. Optical design of these and other applications requires knowledge of the optical constants, in some cases, over the whole solar spectrum. Various optical property measurements were performed including variable angle spectroscopic ellipsometry, and spectral transmittance and reflectance measurements. This material is deposited in several steps and has a fairly complex structure. The measured data were fit to models based on this structure to obtain the optical indices. Atomic force microscopy confirmed the optically modeled surface roughness.

### INTRODUCTION

Doped SnO<sub>2</sub> is besides doped In<sub>2</sub>O<sub>3</sub> and ZnO the best known representative of the class of transparent conductors and finds use in form of poly-crystalline thin films. Its applications include photovoltaic and electrochromic devices, glass coatings for furnace windows, for deicing or defogging as well as transparent electrodes for liquid crystal displays. Metal-oxides often behave like semiconductors with a wide band gap due to their strong chemical bonds. To reduce its resistivity SnO<sub>2</sub> can be doped with fluorine (group VII). In this case F<sup>1-</sup> substitutes O<sup>2-</sup> and therefore acts as an electron donor resulting in a conduction mechanism of the n-type. The specific resistivity of polycrystalline doped SnO<sub>2</sub> can be as low as 10<sup>-3</sup> Ωcm and is limited mainly by low mobility's in the order of 20 cm<sup>2</sup>/Vs<sup>1</sup>, smaller than in single crystals due to impurities, dislocations and grain boundary effects<sup>2</sup>. It shall be stressed that all values reflect an average of published data. Depending on different deposition Techniques and conditions there might be some spread in data as it is shown in numerous publications<sup>3</sup>. The apparent band gap appears in total blue-shifted due to the degenerate doping level. Carrier concentrations in doped SnO<sub>2</sub> are lower than in In<sub>2</sub>O<sub>3</sub>:Sn (ITO) by almost a factor of two, because the solubility of fluorine in SnO<sub>2</sub> is inferior to that of Sn in In<sub>2</sub>O<sub>3</sub><sup>1</sup>. This results in a lower infrared reflectivity and higher resistance of SnO<sub>2</sub>:F. Despite these drawbacks the lower costs make it an interesting alternative for applications, where large areas have to be coated. This is especially the case for heat mirror applications or for displays. Furthermore it is chemically quite stable which enables outdoor use as window coating. At the same time this property allows a wide variety of deposition Techniques and direct application of various coatings.

The commercially available transparent conductive substrates Tech20 and Tech15 glass by Libbey Owens Ford are commonly referred to as tin-oxide glass, but they are in reality multilayer structures composed by different materials. On a soda-lime-silicate (glass) substrate a thin intrinsic SnO<sub>2</sub> layer is deposited. It is followed by a thin SiO<sub>2</sub> film and finally the thick SnO<sub>2</sub>:F layer. The numbers 20 and 15 refer to the nominal sheet resistance of 20 Ω/□ and 15 Ω/□

respectively, where the sheet resistance is defined as the ratio of specific resistivity and film thickness.

## METHODS

The optical properties are measured using both ellipsometric and radiometric Techniques. A variable-angle spectroscopic ellipsometer by J.A Woollam Co. is used over the extended visible range (290-1000 nm). An averaging over 60 revolutions of the analyzer unit of the ellipsometer was found to be sufficient to reduce the noise level significantly. The choice of angles 59°, 62° and 65° yielded values of  $\Psi$  and  $\Delta$  that were lying near the region of optimum sensitivity for our rotating analyzer ellipsometer over the whole spectral range<sup>4</sup>.

Transmittance and reflectance measurements are made over the solar spectrum from 290-2500 nm. Transmittance measurements were made at normal incidence using a Perkin-Elmer Lambda 19 spectrophotometer. Reflectance measurements were made with relative reflectance attachment with an angle of incidence of 8 degrees. A front-surface Al mirror calibrated by NIST was used as a reference.

Some of the surface features of the structural model were verified by atomic force microscopy (AFM) using a Park Scientific Instruments Autoprobe.

Ellipsometric and radiometric data were fitted together weighting both data types according to their experimental standard deviations. The standard deviations of the reflectance and transmittance measurements were not directly measured. They had to be assigned by comparison of repeated measurements over the whole spectral range from 290-2500 nm to 0.1% for transmittance and 0.2% for reflectance data respectively. Backside reflections were generally accounted for and included as fit parameters.

## RESULTS

Ellipsometric and radiometric data (Figure 1 through Figure 4) were taken from a sample of Tech15 glass from Libbey Owens Ford Corporation made by pyrolytic CVD.

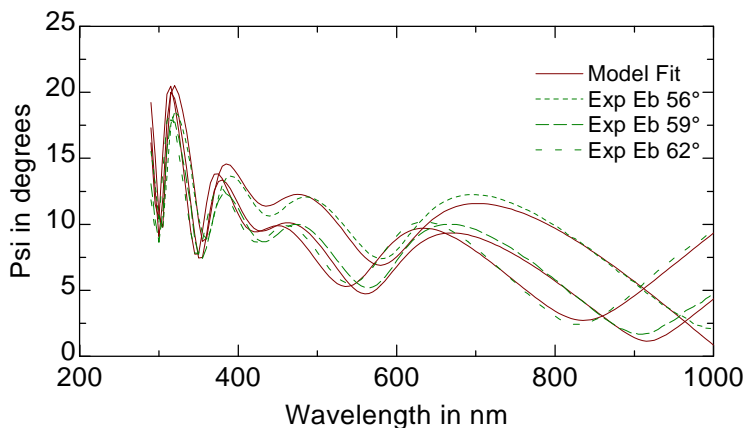


Figure 1. Spectral ellipsometric  $\psi$ -data at 3 angles (dashed lines) for Tech15 glass and fitted by the model of Figure 6 (solid lines).

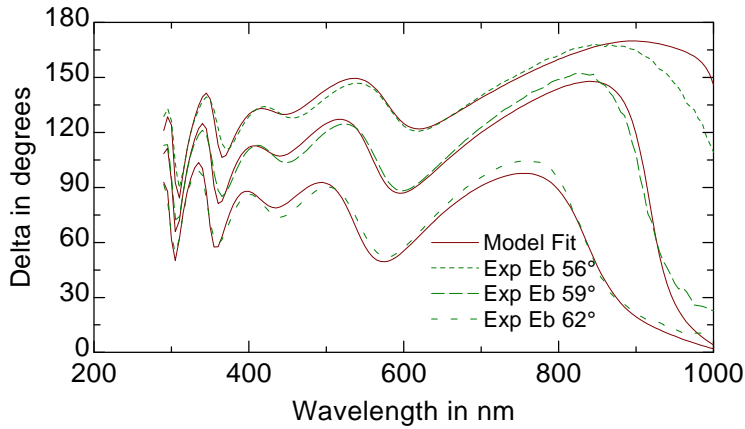


Figure 2. Spectral ellipsometric  $\Delta$ -data at 3 angles (dashed lines) for Tech15 glass and fitted by the model of Figure 6 (solid lines).

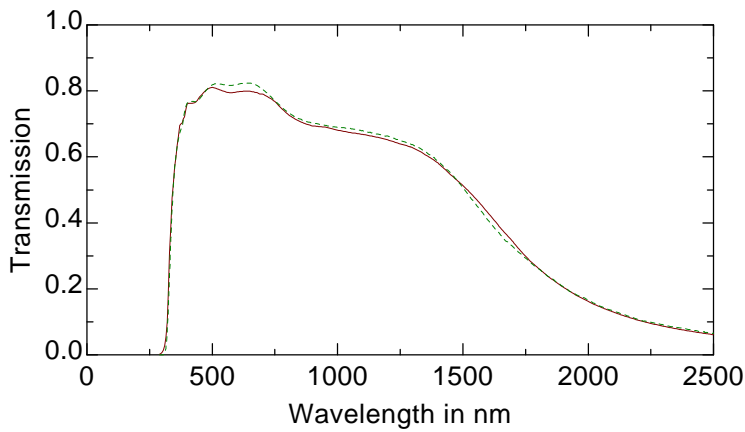


Figure 3. Spectral transmittance data at normal incidence (dashed line) for Tech15 glass, and fitted by the model of Figure 6 (solid line).

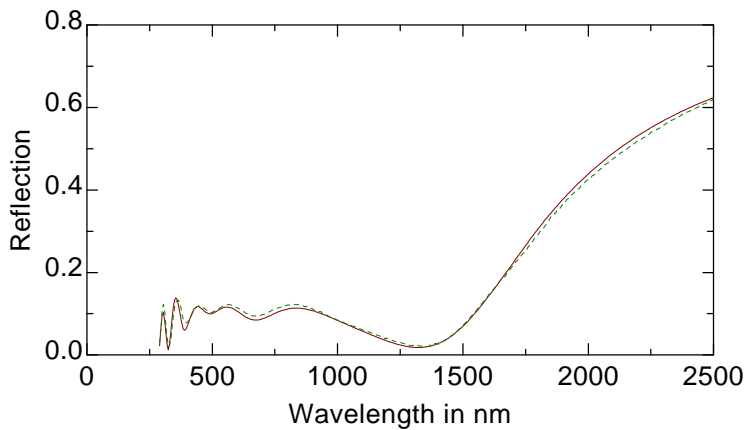


Figure 4. Spectral reflectance data at  $8^\circ$  incidence (dashed line) for Tech15 glass, and fitted by the model of Figure 6 (solid line).

It shall be pointed out that a perfect match of calculated and experimental transmittance data is possible by only slightly varying the extinction coefficient  $k$  around the predicted values by the dispersion model. Yet it is astonishing by itself how good the fit of the purely physical model already is. Even the differences in transmittance data around 550nm lie still within 2%.

It is complicated to extract uncorrelated information out of a multilayer structure. To obtain information about an underlying layer it is naturally necessary that the overlying films are transparent over the whole spectral range where information is desired. Sometimes it is therefore very practical to deposit those layers as a single film on a well characterized and easy-to-measure substrate. But the optical properties of an isolated thin film can be significantly different from those of a film within a stack. Growth conditions for the overlying layers can change the original single film significantly and the contact of two different materials can have influence as well.

One major problem of fitting the experimental data to a structural model was the correlation of the thickness of the bottom  $\text{SnO}_2$  layer and its covering film of  $\text{SiO}_2$ . But by carefully varying only one thickness when the other one was kept fixed, a shallow minimum of the mean square error was found extending over about 5 nm of the thickness of the  $\text{SiO}_2$  layer indicating thickness in-homogeneity or an irregular interface.

ema ( $\text{SnO}_2\text{:F}$ )/50% void	27 nm
$\text{SnO}_2\text{:F}$	226 nm
$\text{SiO}_2$	27 nm
$\text{SnO}_2$	24 nm
glass	3 mm

Figure 5. Structural model for Tech20 glass

ema ( $\text{SnO}_2\text{:F}$ )/50% void	31 nm
$\text{SnO}_2\text{:F}$	292 nm
$\text{SiO}_2$	20 nm
$\text{SnO}_2$	30 nm
glass	3 mm

Figure 6. Structural model for Tech15 glass.

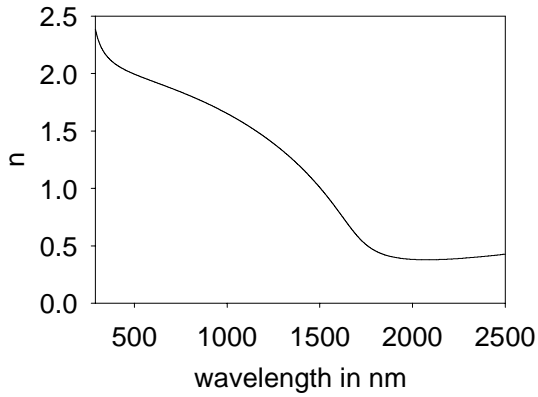
One Lorentz oscillator in the UV could adequately represent the dispersion of the intrinsic  $\text{SnO}_2$  layer over the wavelength range of the solar spectrum, whereas a Drude free electron component had to be added to the fluorine doped layer.

Undoped  $\text{SnO}_2$  is a defect compound tending to form numerous oxygen vacancies resulting in carrier concentrations of  $10^{17}$ - $10^{19}$   $\text{cm}^{-3}$ . Although the conductivity is much smaller than that of  $\text{SnO}_2\text{:F}$ , the free electron influence should nevertheless be observable. It must be pointed out that the  $\text{SnO}_2\text{:F}$  layer turns opaque above 1.5  $\mu\text{m}$  due to its free carriers' influence. There is a sharp increase of the extinction coefficient near the plasma wavelength at 1720 nm in the near infrared (Figure 7b). Therefore in this spectral region optical information about the underlying  $\text{SnO}_2$  film is only obtainable from the reverse side through the glass substrate. Reflectance measurements did not reveal significant influence of free carriers below 2500 nm.

It should be assumed that there could be a similar phenomenon of depth dependent dispersion in  $\text{SnO}_2\text{:F}$  like in ITO<sup>5</sup>. But already a simple model consisting out of one

homogeneous layer can provide good agreement between calculated and measured data. Therefore the effect in SnO<sub>2</sub>:F seems to be at least less dominant than in ITO. Trying to split the SnO<sub>2</sub>:F layer into several layers did not improve the fit significantly, but lead to important fit parameter correlation which indicates that no essential improvement in representation of physical reality was made by this approach.

a)



b)

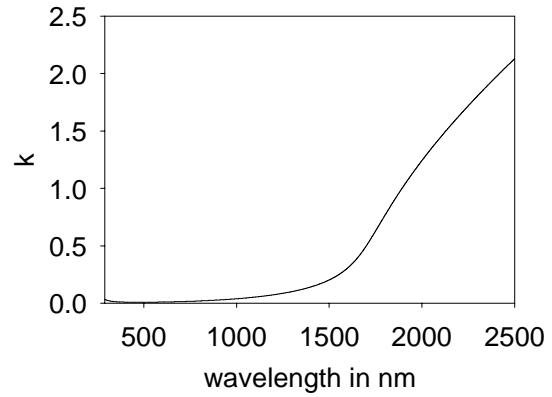
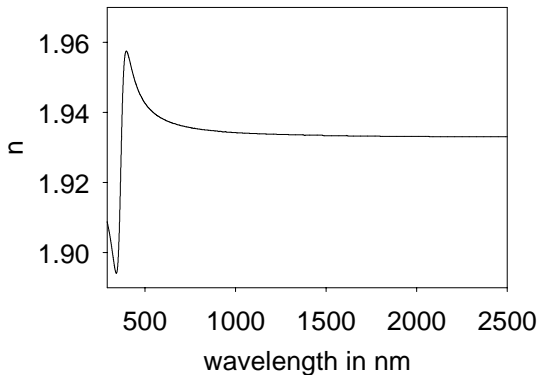


Figure 7. a) Real part  $n$  and b) imaginary part  $k$  of the refractive index for SnO<sub>2</sub>:F

a)



b)

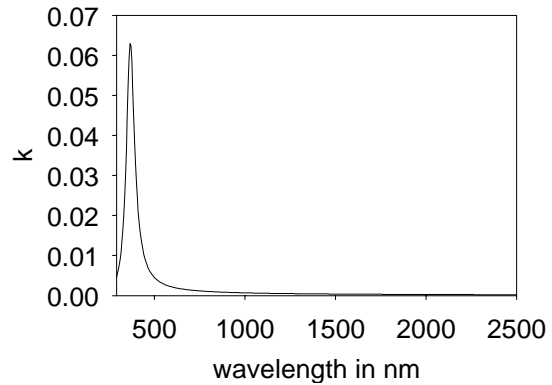


Figure 8. a) Real part  $n$  and b) imaginary part  $k$  of the refractive index for SnO<sub>2</sub>

Optical indices can be calculated from a Drude-Lorentz dispersion model:

$$\tilde{\epsilon}(E) = \epsilon_{\infty} - \frac{A_D}{E^2 + i\Gamma_D E} + \frac{A_L}{E_L^2 - E^2 - i\Gamma_L E} \quad (1)$$

Best fit parameters are tabulated below (Table 1).

	$\epsilon_\infty$	$A_D$ [eV <sup>2</sup> ]	$\Gamma_D$ [eV]	$A_L$ [eV <sup>2</sup> ]	$\Gamma_L$ [eV]	$E_L$ [eV]
SnO <sub>2</sub>	3.70	-	-	0.417	0.5064	3.386
SnO <sub>2</sub> :F	3.19	2.173	0.167	24.67	0.1275	5.26

Table 1. Drude and Lorentz parameters of the dispersion model for SnO<sub>2</sub> and SnO<sub>2</sub>:F

Surface roughness was simulated by a Bruggemann effective medium approximation layer, where a portion of 50% void was included to the SnO<sub>2</sub>:F top layer. The complex dielectric constant of this EMA layer can be calculated by numerically solving following equation:

$$\frac{\tilde{\epsilon}_{SnO_2:F} - \tilde{\epsilon}}{\tilde{\epsilon}_{SnO_2:F} + 2\tilde{\epsilon}} + \frac{\tilde{\epsilon}_{void} - \tilde{\epsilon}}{\tilde{\epsilon}_{void} + 2\tilde{\epsilon}} = 0 \quad (2)$$

Such a layer added to the model significantly improves the fit and results in a surface roughness of 27 nm for Tech20 and 31 nm for Tech15 glass in close agreement with direct AFM measurement.

## CONCLUSION

Fluorine doped tin-oxide was found to be governed by its free electron properties in the infrared while it exhibits the features of a wide band gap semiconductor in the UV and lower part of the visible.

The undoped SnO<sub>2</sub> film shows behavior of a wide band gap semiconductor with absorption at the band edge in the UV and dielectric behavior in the visible and near IR.

Improved results can be obtained by considering surface roughness.

## ACKNOWLEDGMENT

Special thanks to Peter Gerhardinger of Libbey Owens Ford Corporation for providing sample materials and Technical information.

This work was supported by the Assistant Secretary for Energy Efficiency and Renewable Energy, Office of Building Technologies, Building Systems and Materials Division of the US Department of Energy under Contract No. DE-AC03-76SF00098.

## DISCLAIMER

This document was prepared as an account of work sponsored by the United States Government. While this document is believed to contain correct information, neither the United States Government nor any agency thereof, nor The Regents of the University of California, nor any of their employees, makes any warranty, express or implied, or assumes any legal responsibility for the accuracy, completeness, or usefulness of any information, apparatus, product, or process disclosed, or represents that its use would not infringe privately owned rights. Reference herein to any specific commercial product, process, or service by its trade name, trademark, manufacturer, or otherwise, does not necessarily constitute or imply its endorsement, recommendation, or favoring by the United States Government or any agency thereof, or The Regents of the University of California. The views and opinions of authors expressed herein do not necessarily state or reflect those of the United States Government or any agency thereof, or The Regents of the University of California.

---

## REFERENCES

- <sup>1</sup> H. Köstlin, Festkörperprobleme **XXII** (1982)
- <sup>2</sup> M. Misonou and K. Kawahara, SPIE IS **4**, 402
- <sup>3</sup> C. Lampert, Sol. En. Mat. **6** (1981)
- <sup>4</sup> J. A. Woollam Co., WVASE32, (1995)
- <sup>5</sup> K. von Rottkay, M. Rubin, N. Ozer, presented at the 1995 MRS Fall Meeting, Boston, MA, 1995 (unpublished)